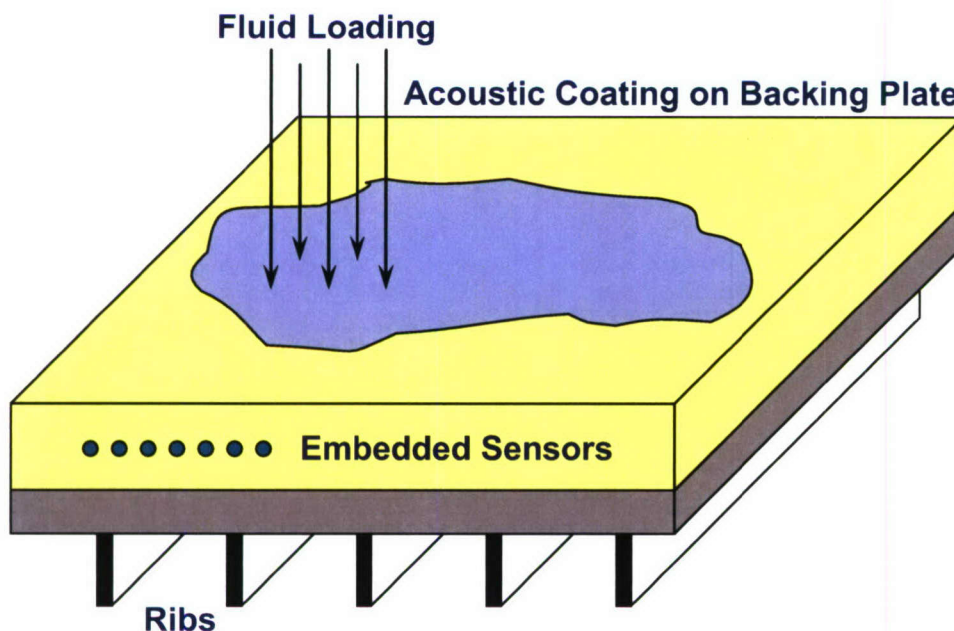


# Response of an Acoustic Coating on a Rib-Stiffened Plate

Andrew J. Hull  
John R. Welch  
Autonomous and Defensive Systems Department



Naval Undersea Warfare Center Division  
Newport, Rhode Island

Approved for public release; distribution is unlimited.

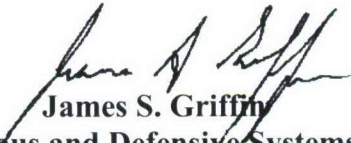
20080924037

## **PREFACE**

The work described in this report was sponsored by the Naval Undersea Warfare Center (NUWC) Virtual In-House Laboratory Independent Research (ILIR) Program under the project entitled "Modeling and Analysis of Fully-Elastic Periodic Structures," NUWC Job Order Number N625548.

The technical reviewer for this report was Benjamin A. Cray (Code 821).

**Reviewed and Approved: 6 June 2008**



**James S. Griffin**  
**Head, Autonomous and Defensive Systems Department**



<b>REPORT DOCUMENTATION PAGE</b>				Form Approved OMB No. 0704-0188	
The public reporting burden for this collection of information is estimated to average 1 hour per response, including the time for reviewing instructions, searching existing data sources, gathering and maintaining the data needed, and completing and reviewing the collection of information. Send comments regarding this burden estimate or any other aspect of this collection of information, including suggestions for reducing this burden, to Department of Defense, Washington Headquarters Services, Directorate for Information Operations and Reports (0704-0188), 1215 Jefferson Davis Highway, Suite 1204, Arlington, VA 22202-4302. Respondents should be aware that notwithstanding any other provision of law, no person shall be subject to any penalty for failing to comply with a collection of information if it does not display a currently valid OPM control number. <b>PLEASE DO NOT RETURN YOUR FORM TO THE ABOVE ADDRESS.</b>					
1. REPORT DATE (DD-MM-YYYY) 06-06-2008		2. REPORT TYPE Final		3. DATES COVERED (From - To)	
4. TITLE AND SUBTITLE  Response of an Acoustic Coating on a Rib-Stiffened Plate				5a. CONTRACT NUMBER	
				5b. GRANT NUMBER	
				5c. PROGRAM ELEMENT NUMBER	
6. AUTHOR(S)  Andrew J. Hull John R. Welch				5d. PROJECT NUMBER	
				5e. TASK NUMBER	
				5f. WORK UNIT NUMBER	
7. PERFORMING ORGANIZATION NAME(S) AND ADDRESS(ES)  Naval Undersea Warfare Center Division 1176 Howell Street Newport, RI 02841-1708				8. PERFORMING ORGANIZATION REPORT NUMBER  TR 11859	
9. SPONSORING/MONITORING AGENCY NAME(S) AND ADDRESS(ES)				10. SPONSORING/MONITOR'S ACRONYM	
				11. SPONSORING/MONITORING REPORT NUMBER	
12. DISTRIBUTION/AVAILABILITY STATEMENT  Approved for public release; distribution is unlimited.					
13. SUPPLEMENTARY NOTES					
14. ABSTRACT This report develops an analytical model of a fluid-loaded acoustic coating affixed to a rib-stiffened plate. The model is three-dimensional and has fully-elastic behavior. The system is loaded by a plane wave that is harmonic both spatially and temporally. The model begins with Naviers' equations of motion of an elastic solid, which produces unknown displacement fields that are inserted in to stress equations at the boundaries of the plate and the acoustic coating. These stress fields are coupled to the fluid field and the rib stiffeners with force balances. Manipulation of these equations develops an infinite number of indexed equations that are truncated and incorporated into a global matrix equation. This global matrix equation can be solved, and the result is the system displacements, stresses, and scattered pressure field. This problem is investigated for two specific outputs: (1) a sonar array embedded in the acoustic coating and (2) the scattered pressure field. The results are compared to previously developed models for the system without ribs. It is shown that the ribs can have a significant impact on stresses in the acoustic coating and the scattered pressure field.					
15. SUBJECT TERMS Acoustic Coating      Embedded Sensors      Fluid Loaded      Rib-Stiffened Plate      Sonar Array					
16. SECURITY CLASSIFICATION OF:			17. LIMITATION OF ABSTRACT	18. NUMBER OF PAGES  45	19a. NAME OF RESPONSIBLE PERSON Andrew J. Hull
a. REPORT (U)	b. ABSTRACT (U)	c. THIS PAGE (U)			19b. TELEPHONE NUMBER (Include area code) (401) 832-5189



## TABLE OF CONTENTS

Section	Page
1 INTRODUCTION .....	1
2 SYSTEM MODEL .....	3
3 ANALYTICAL SOLUTION.....	9
4 MODEL VALIDATION .....	19
5 AN EXAMPLE PROBLEM.....	23
6 CONCLUSIONS .....	29
7 REFERENCES .....	31
APPENDIX—MATRIX AND VECTOR ENTRIES.....	A-1

## LIST OF ILLUSTRATIONS

Figure	Page
1 Schematic of Plate System Showing Coordinate System .....	3
2 Transfer Function Magnitude of Normal Displacement Divided by Incident Pressure at 10 Hz with $k_y = 2 \text{ rad m}^{-1}$ (top) and $k_x = 2 \text{ rad m}^{-1}$ (bottom) for Thick Plate System ( ____ ) and Thin Plate System ( • ).....	22
3 Transfer Function Magnitude of Average Stress Divided by Incident Pressure at 8027 Hz with $\phi = 0^\circ$ (top) and $\phi = 45^\circ$ (bottom) for the System with Ribs at $x = 0$ ( ____ ) , $x = L/2$ ( ____ ) and System without Ribs at any $x$ Value ( - - - - ).....	24
4 Summed Acoustic Array Response with a Steer Angle of $0^\circ$ (top) and $-45^\circ$ (bottom) for the System with Ribs ( ____ ) and System without Ribs ( - - - - ) at 8027 Hz.....	26
5 Transfer Function Magnitude of Scattered Pressure Divided by Incident Pressure at 8027 Hz with $\phi = 0^\circ$ (top) and $\phi = 45^\circ$ (bottom) for the System with Ribs at $x = 0$ ( ____ ) , $x = L/2$ ( ____ ) and System without Ribs at any $x$ Value ( - - - - ).....	28



# RESPONSE OF AN ACOUSTIC COATING ON A RIB-STIFFENED PLATE

## 1. INTRODUCTION

Underwater vehicle hulls are typically metallic with acoustic coatings that are made of a polymer material. These hulls are usually internally reinforced in one direction to provide increased stiffness against the hydrostatic forces that act on the hull when the vessel is submerged. Acoustic coatings are used to produce quieter vehicles, contain sonar sensors, inhibit drag, and prevent biological fouling on the exterior of the vehicle. Understanding the structural response of such a system is important for the design of new underwater vehicles and analysis of existing underwater vehicles. An analytical model of this type of configuration will allow predictions of the dynamic response of an acoustic coating on a marine structure and any sonar system that is embedded in the coating.

The research of plate theory has been an ongoing field of study for many years. Thin beam (Euler-Bernoulli) theory originates in the eighteenth century.<sup>1</sup> This model is sometimes called a flexural wave model, and an extremely similar model exists in plate theory. Mindlin<sup>2</sup> modified thin plate theory to include the dynamics of rotary inertia and shear effects, and this extended the low wavenumber accuracy of the model. Analysis of wave propagation in fully-elastic plates consisting of one or multiple layers using Naviers' equations of motion has been studied extensively and is well documented.<sup>3</sup> Fluid loading has been added to thin plate analysis<sup>4</sup> and thick plate single and multilayer analysis.<sup>5</sup> Using these techniques, the dynamic response of fluid-loaded acoustic coating on an unreinforced plate can be calculated and analyzed.

Over the years, plate theory has been expanded to include stiffening effects of ribs that are typical of many marine and aviation structures. They are almost inclusively placed on one side of the plate to reinforce the structure. The response of a periodically supported beam to a load with fixed wavenumber and frequency has been investigated.<sup>6</sup> The response of periodically stiffened fluid-loaded plates to harmonic loading<sup>7</sup> and line and point forces<sup>8</sup> has been established. The problem of aperiodicity in the stiffeners has been solved.<sup>9</sup> This problem was also investigated for a finite number of equally-spaced stiffeners<sup>10</sup> and randomly spaced stiffeners.<sup>11</sup> Asymptotic models of plate radiation into fluid fields have also been developed.<sup>12</sup> It is noted that

these papers<sup>6-12</sup> use some form of thin plate theory, and the resulting frequency limit where the model assumptions are valid depends on the thickness of the plate, but for most plates it is typically in the hundreds of Hertz. The acoustic response of a fully-elastic cylindrical shell with a complete acoustic coating has been researched<sup>13</sup> as well as that of a cylindrical shell with a partial acoustic coating.<sup>14</sup> There are no rib effects present in either of these papers. Higher frequency analysis is possible using numerical methods such as finite element analysis;<sup>15</sup> however, these computations can be time consuming and frequently have stability problems when Poisson's ratio of the coating material approaches 0.5. Recently, a fully-elastic solution to a plate containing discrete masses was developed.<sup>16</sup> This method can be extended to model the behavior of an acoustic coating on a ribbed backing plate.

This report presents an analytical model of a plate in contact with a fluid-loaded acoustic coating on one side and a series of equally spaced ribs on the other side. The structure is loaded through the fluid with an incoming acoustic wave. The plate and the acoustic coating are modeled as three-dimensional fully-elastic solid bodies, the fluid is modeled as a three-dimensional acoustic field, and the ribs are modeled as discrete springs. The formulation begins with elasticity theory where the motion in the plate and the acoustic coating are modeled as a combination of dilatational and shear waves. These waveforms can be used to determine the three-dimensional displacement fields with unknown coefficients. These displacements are inserted into stress and continuity equations at the system boundaries and interfaces that contain the system excitation, the fluid loading, and the force of the ribs on the structure. Using an orthogonalization procedure produces an  $m$ -indexed mathematical model of the system where each  $m$  index is a set of equations twelve rows by an infinite number of columns. All of the  $m$ -indexed equations can be combined and this yields a matrix system of infinite extent, which is truncated to a finite number of lower wavenumber terms. Inverting this matrix solves for the unknown coefficients and produces system displacements, stresses, and pressure field solutions. The fully-elastic model is compared to a previously developed thin plate model at low frequency and wavenumbers to insure accuracy and consistency to prior work. A numerical example problem is then studied with specific interest in reception of acoustic signals and strength of the scattered field. It is shown that the ribs can moderately affect the system response.



## 2. SYSTEM MODEL

The system model is that of a fluid-loaded solid layer, called the acoustic coating, in contact with a rib-stiffened solid layer, called the backing plate, as shown in figure 1. This problem is analytically modeled by assuming that the pressure in the fluid is governed by the acoustic wave equation, both solid layers are governed by fully-elastic equations of motion, and the rib stiffeners are modeled as discrete linear springs. The acoustic coating is loaded on the top surface with an incoming acoustic wave. The ribs on the bottom of the backing plate are equally spaced at a distance of  $L$  (m) in the  $x$ -direction and each has stiffness per unit length of  $K$  ( $\text{Nm}^{-2}$ ). The model uses the following assumptions: (1) the forcing function acting on the plate is a plane wave at definite wavenumbers in the  $x$ - and  $y$ -directions and frequency in time, (2) motion in both plates is normal in the  $z$ -direction and tangential in the  $x$ - and  $y$ -directions (three-dimensional system), (3) both plates have infinite spatial extent in the  $x$ - and  $y$ -directions, (4) at the interface of the acoustic coating and backing plate, the surfaces move in contact with one another and the stresses are equivalent, (5) the ribs are modeled as springs that have translational degrees of freedom in the  $z$ -direction, (6) the particle motion is linear, and (7) the fluid medium is lossless.

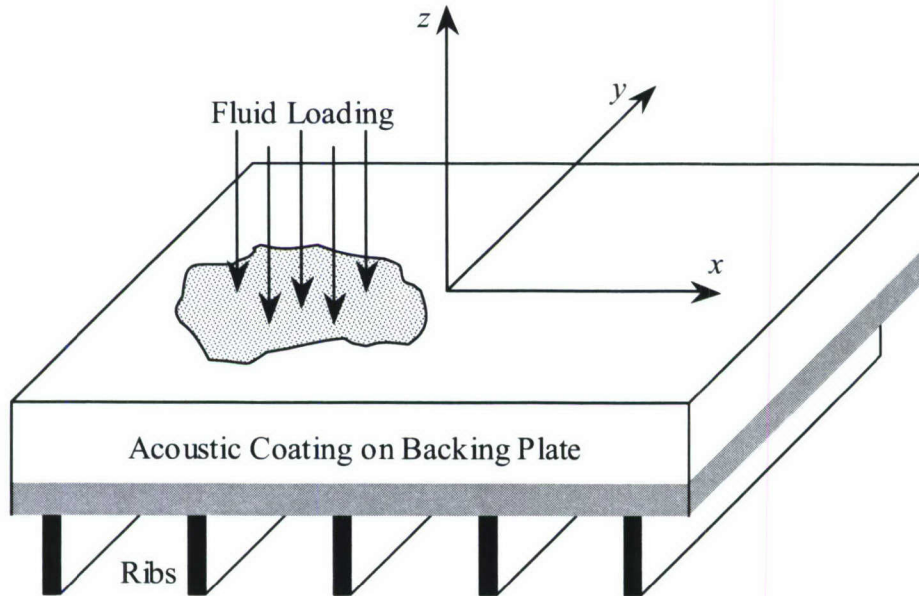


**Figure 1. Schematic of Plate System Showing Coordinate System**



The motions of both the backing plate and the acoustic coating are governed the Naviers' equations of motion written in vector form as

$$\mu \nabla^2 \mathbf{u}(x, y, z, t) + (\lambda + \mu) \nabla \nabla \cdot \mathbf{u}(x, y, z, t) = \rho \frac{\partial^2 \mathbf{u}(x, y, z, t)}{\partial t^2}, \quad (1)$$

where  $\rho$  is the density ( $\text{kg m}^{-3}$ ),  $\lambda$  and  $\mu$  are the complex Lamé constants ( $\text{N m}^{-2}$ ),  $t$  is time (seconds),  $\cdot$  denotes a vector dot product, and  $\mathbf{u}(x, y, z, t)$  is the three-dimensional Cartesian coordinate displacement vector and is written as

$$\begin{aligned} \mathbf{u}(x, y, z, t) &= [u(x, y, z, t) \quad v(x, y, z, t) \quad w(x, y, z, t)]^T \\ &= \nabla \phi(x, y, z, t) + \nabla \times \vec{\psi}(x, y, z, t), \end{aligned} \quad (2)$$

where  $\phi$  is a dilatational scalar potential,  $\nabla$  is the gradient operator,  $\times$  denotes a vector crossproduct, and  $\vec{\psi}$  is an equivoluminal vector potential given by

$$\vec{\psi}(x, y, z, t) = [\psi_x(x, y, z, t) \quad \psi_y(x, y, z, t) \quad \psi_z(x, y, z, t)]^T. \quad (3)$$

Additionally, the constraint equation on the equivoluminal vector potential is

$$\nabla \cdot \vec{\psi}(x, y, z, t) = 0. \quad (4)$$

Expanding equation (2) gives the individual displacements as

$$u(x, y, z, t) = \frac{\partial \phi(x, y, z, t)}{\partial x} + \frac{\partial \psi_z(x, y, z, t)}{\partial y} - \frac{\partial \psi_y(x, y, z, t)}{\partial z}, \quad (5)$$

$$v(x, y, z, t) = \frac{\partial \phi(x, y, z, t)}{\partial y} - \frac{\partial \psi_z(x, y, z, t)}{\partial x} + \frac{\partial \psi_x(x, y, z, t)}{\partial z}, \quad (6)$$

and

$$w(x, y, z, t) = \frac{\partial \phi(x, y, z, t)}{\partial z} + \frac{\partial \psi_y(x, y, z, t)}{\partial x} - \frac{\partial \psi_x(x, y, z, t)}{\partial y}. \quad (7)$$

Equations (5), (6), and (7) are next inserted into equation (1), which results in four decoupled wave equations, given by

$$c_d^2 \nabla^2 \phi(x, y, z, t) = \frac{\partial^2 \phi(x, y, z, t)}{\partial t^2}, \quad (8)$$

$$c_s^2 \nabla^2 \psi_x(x, y, z, t) = \frac{\partial^2 \psi_x(x, y, z, t)}{\partial t^2}, \quad (9)$$

$$c_s^2 \nabla^2 \psi_y(x, y, z, t) = \frac{\partial^2 \psi_y(x, y, z, t)}{\partial t^2}, \quad (10)$$

$$c_s^2 \nabla^2 \psi_z(x, y, z, t) = \frac{\partial^2 \psi_z(x, y, z, t)}{\partial t^2}, \quad (11)$$

where equation (8) corresponds to the dilatational component and equations (9), (10), and (11) correspond to the shear component of the displacement field. Correspondingly, the constants  $c_d$  and  $c_s$  are the complex dilatational and shear wave speeds ( $\text{m s}^{-1}$ ), respectively, and are determined by

$$c_d = \sqrt{\frac{\lambda + 2\mu}{\rho}} \quad (12)$$

and

$$c_s = \sqrt{\frac{\mu}{\rho}}. \quad (13)$$

The system equations of motion are formulated as a boundary value problem using twelve equations of stress and displacement continuity written in terms of the plates' displacements and corresponding forcing functions. The system is loaded on the bottom by the springs acting in the  $z$ -direction; thus, the normal stress at this location ( $z = a$ ) is written using a force balance between the springs and the lower plate as

$$\begin{aligned} \tau_{zz}(x, y, a, t) &= \lambda_1 \left[ \frac{\partial u_1(x, y, a, t)}{\partial x} + \frac{\partial v_1(x, y, a, t)}{\partial y} + \frac{\partial w_1(x, y, a, t)}{\partial z} \right] + 2\mu_1 \frac{\partial w_1(x, y, a, t)}{\partial z} \\ &= \sum_{n=-\infty}^{n=+\infty} K w_1(x, y, a, t) \delta(x - nL), \end{aligned} \quad (14)$$

where  $\delta(x - nL)$  is the spatial Dirac delta function that distributes the force of the springs discretely and equally spaced in the  $x$ -direction and the subscript 1 corresponds to the backing plate. The tangential stresses at the bottom of the backing plate are zero and are written as

$$\tau_{zy}(x, y, a, t) = \mu_1 \left[ \frac{\partial v_1(x, y, a, t)}{\partial z} + \frac{\partial w_1(x, y, a, t)}{\partial y} \right] = 0 \quad (15)$$

and

$$\tau_{zx}(x, y, a, t) = \mu_1 \left[ \frac{\partial w_1(x, y, a, t)}{\partial x} + \frac{\partial u_1(x, y, a, t)}{\partial z} \right] = 0. \quad (16)$$

The interface between the backing plate and the acoustic coating is modeled using continuity of displacements and stresses. Continuity of the stress fields at the interface ( $z = b$ ) yields



$$\lambda_1 \left[ \frac{\partial u_1(x, y, b, t)}{\partial x} + \frac{\partial v_1(x, y, b, t)}{\partial y} + \frac{\partial w_1(x, y, b, t)}{\partial z} \right] + 2\mu_1 \frac{\partial w_1(x, y, b, t)}{\partial z} = \lambda_2 \left[ \frac{\partial u_2(x, y, b, t)}{\partial x} + \frac{\partial v_2(x, y, b, t)}{\partial y} + \frac{\partial w_2(x, y, b, t)}{\partial z} \right] + 2\mu_2 \frac{\partial w_2(x, y, b, t)}{\partial z}, \quad (17)$$

$$\mu_1 \left[ \frac{\partial v_1(x, y, b, t)}{\partial z} + \frac{\partial w_1(x, y, b, t)}{\partial y} \right] = \mu_2 \left[ \frac{\partial v_2(x, y, b, t)}{\partial z} + \frac{\partial w_2(x, y, b, t)}{\partial y} \right], \quad (18)$$

and

$$\mu_1 \left[ \frac{\partial w_1(x, y, b, t)}{\partial x} + \frac{\partial u_1(x, y, b, t)}{\partial z} \right] = \mu_2 \left[ \frac{\partial w_2(x, y, b, t)}{\partial x} + \frac{\partial u_2(x, y, b, t)}{\partial z} \right]. \quad (19)$$

The subscript 2 corresponds to the acoustic coating. Continuity of the displacement fields at the interface yields

$$u_1(x, y, b, t) = u_2(x, y, b, t), \quad (20)$$

$$v_1(x, y, b, t) = v_2(x, y, b, t), \quad (21)$$

and

$$w_1(x, y, b, t) = w_2(x, y, b, t). \quad (22)$$

The top of the acoustic coating is in contact with a fluid, and the normal stress at this location ( $z = c$ ) is written using a force balance between the pressure in the fluid and the coating as

$$\begin{aligned} \tau_{zz}(x, y, c, t) &= \lambda_2 \left[ \frac{\partial u_2(x, y, c, t)}{\partial x} + \frac{\partial v_2(x, y, c, t)}{\partial y} + \frac{\partial w_2(x, y, c, t)}{\partial z} \right] + 2\mu_2 \frac{\partial w_2(x, y, c, t)}{\partial z} \\ &= -p_a(x, y, c, t), \end{aligned} \quad (23)$$

where  $p_a(x, y, c, t)$  is the pressure field in contact with the top of the plate ( $\text{N m}^{-2}$ ). The tangential stresses on the top of the acoustic coating are modeled as free boundary conditions and are written as

$$\tau_{zy}(x, y, c, t) = \mu_2 \left[ \frac{\partial v_2(x, y, c, t)}{\partial z} + \frac{\partial w_2(x, y, c, t)}{\partial y} \right] = 0 \quad (24)$$

and

$$\tau_{zx}(x, y, c, t) = \mu_2 \left[ \frac{\partial w_2(x, y, c, t)}{\partial x} + \frac{\partial u_2(x, y, c, t)}{\partial z} \right] = 0. \quad (25)$$

The acoustic pressure in the fluid medium is governed by the three-dimensional wave equation and is written in Cartesian coordinates as

$$\frac{\partial^2 p_a(x, y, z, t)}{\partial x^2} + \frac{\partial^2 p_a(x, y, z, t)}{\partial y^2} + \frac{\partial^2 p_a(x, y, z, t)}{\partial z^2} - \frac{1}{c_f^2} \frac{\partial^2 p_a(x, y, z, t)}{\partial t^2} = 0, \quad (26)$$

where  $p_a(x, y, z, t)$  is the pressure ( $\text{N m}^{-2}$ ) and  $c_f$  is the real-valued compressional wavespeed in the fluid ( $\text{m s}^{-1}$ ). The interface between the fluid and the top of the acoustic coating ( $z = c$ ) satisfies the linear momentum equation, which relates the normal acceleration of the plate surface to the spatial gradient of the pressure field by

$$\rho_f \frac{\partial^2 w_2(x, y, c, t)}{\partial t^2} = - \frac{\partial p_a(x, y, c, t)}{\partial z}, \quad (27)$$

where  $\rho_f$  is the density of the fluid ( $\text{kg m}^{-3}$ ).

### 3. ANALYTICAL SOLUTION

All three displacements are now determined by solving equations (8), (9), (10), and (11), inserting these results into equations (5), (6), and (7), and applying equation (4) to eliminate two of the resulting constants. Because of the periodicity in the  $x$ -direction, the functional form of the displacements are equal to the sum of an unknown function in the  $z$ -direction, which is multiplied by an indexed exponential function in the  $x$ -direction, by an exponential function in the  $y$ -direction, and by an exponential function in time. Others note this functional form and discuss its derivation.<sup>6</sup> This is written as

$$u_j(x, y, z, t) = \sum_{m=-\infty}^{m=+\infty} U_m^{(j)}(z) \exp(ik_m x) \exp(ik_y y) \exp(-i\omega t), \quad (28)$$

$$v_j(x, y, z, t) = \sum_{m=-\infty}^{m=+\infty} V_m^{(j)}(z) \exp(ik_m x) \exp(ik_y y) \exp(-i\omega t), \quad (29)$$

and

$$w_j(x, y, z, t) = \sum_{m=-\infty}^{m=+\infty} W_m^{(j)}(z) \exp(ik_m x) \exp(ik_y y) \exp(-i\omega t) \quad (30)$$

where  $i = \sqrt{-1}$ ,  $\omega$  is frequency ( $\text{rad s}^{-1}$ ),  $j$  is either 1, which corresponds to the backing plate or 2, which corresponds to the acoustic coating,  $k_y$  is wavenumber with respect to the  $y$ -axis ( $\text{rad m}^{-1}$ ), and

$$k_m = k_x + \frac{2\pi m}{L}, \quad (31)$$

where  $k_x$  is wavenumber with respect to the  $x$ -axis ( $\text{rad m}^{-1}$ ). The functions  $U_m^{(j)}(z)$ ,  $V_m^{(j)}(z)$ , and  $W_m^{(j)}(z)$  are given by



$$\begin{aligned}
U_m^{(j)}(z) = & A_m^{(j)} i k_m \cos[\alpha_m^{(j)} z] + B_m^{(j)} i k_m \sin[\alpha_m^{(j)} z] + \\
& C_m^{(j)} \frac{k_m k_y}{\beta_m^{(j)}} \sin[\beta_m^{(j)} z] - D_m^{(j)} \frac{k_m k_y}{\beta_m^{(j)}} \cos[\beta_m^{(j)} z] + \\
& E_m^{(j)} \left[ \beta_m^{(j)} + \frac{k_y^2}{\beta_m^{(j)}} \right] \sin[\beta_m^{(j)} z] - F_m^{(j)} \left[ \beta_m^{(j)} + \frac{k_y^2}{\beta_m^{(j)}} \right] \cos[\beta_m^{(j)} z],
\end{aligned} \tag{32}$$

$$\begin{aligned}
V_m^{(j)}(z) = & A_m^{(j)} i k_y \cos[\alpha_m^{(j)} z] + B_m^{(j)} i k_y \sin[\alpha_m^{(j)} z] + \\
& - C_m^{(j)} \left[ \beta_m^{(j)} + \frac{k_m^2}{\beta_m^{(j)}} \right] \sin[\beta_m^{(j)} z] + D_m^{(j)} \left[ \beta_m^{(j)} + \frac{k_m^2}{\beta_m^{(j)}} \right] \cos[\beta_m^{(j)} z] + \\
& - E_m^{(j)} \frac{k_m k_y}{\beta_m^{(j)}} \sin[\beta_m^{(j)} z] + F_m^{(j)} \frac{k_m k_y}{\beta_m^{(j)}} \cos[\beta_m^{(j)} z],
\end{aligned} \tag{33}$$

and

$$\begin{aligned}
W_m^{(j)}(z) = & -A_m^{(j)} \alpha_m^{(j)} \sin[\alpha_m^{(j)} z] + B_m^{(j)} \alpha_m^{(j)} \cos[\alpha_m^{(j)} z] + \\
& - C_m^{(j)} i k_y \cos[\beta_m^{(j)} z] - D_m^{(j)} i k_y \sin[\beta_m^{(j)} z] + \\
& + E_m^{(j)} i k_m \cos[\beta_m^{(j)} z] + F_m^{(j)} i k_m \sin[\beta_m^{(j)} z].
\end{aligned} \tag{34}$$

where  $A_m^{(j)}$ ,  $B_m^{(j)}$ ,  $C_m^{(j)}$ ,  $D_m^{(j)}$ ,  $E_m^{(j)}$  and  $F_m^{(j)}$  are unknown complex wave propagation coefficients of the backing plate and acoustic coating,  $\alpha_m^{(j)}$  is the modified wavenumber ( $\text{rad m}^{-1}$ ) associated with the dilatational wave and is expressed as

$$\alpha_m^{(j)} = \sqrt{[k_d^{(j)}]^2 - k_m^2 - k_y^2}, \tag{35}$$

where  $k_d^{(j)}$  is the dilatational wavenumber on the layer ( $j$ ) and is equal to  $\omega / c_d^{(j)}$ ;  $\beta_m^{(j)}$  is the modified wavenumber ( $\text{rad m}^{-1}$ ) associated with the shear wave and is expressed as

$$\beta_m^{(j)} = \sqrt{[k_s^{(j)}]^2 - k_m^2 - k_y^2}, \tag{36}$$

where  $k_s^{(j)}$  is the shear wavenumber on the layer ( $j$ ) and is equal to  $\omega / c_s^{(j)}$ .

The pressure field in the fluid consists of an incoming incident pressure wave applied to the structure at the top ( $z = c$ ) and an outgoing scattered wave that propagates in the positive  $z$ -direction. Using the analytical form for the pressure field of

$$p(x, y, z, t) = \sum_{m=-\infty}^{m=+\infty} P_m(z) \exp(ik_m x) \exp(ik_y y) \exp(-i\omega t), \quad (37)$$

results in the solution of equation (26) where

$$P_m(z) = R_m \exp(i\gamma_m z) + \delta_{m0} P_I \exp(-i\gamma_m z), \quad (38)$$

where  $\delta_{m0}$  is the Kronecker delta function,  $P_I$  is the magnitude of the applied pressure field ( $\text{N m}^{-2}$ ), and  $\gamma_m$  is the modified wavenumber ( $\text{rad m}^{-1}$ ) associated with the compressional wave in the fluid and is given by

$$\gamma_m = \sqrt{(\omega / c_f)^2 - k_m^2 - k_y^2} = \sqrt{k_f^2 - k_m^2 - k_y^2}. \quad (39)$$

The relationship between arrival angles on the plate of an acoustic wave and the  $x$ - and  $y$ -wavenumbers is determined by

$$k_x = (\omega / c_f) \sin(\theta) \quad (40)$$

and

$$k_y = (\omega / c_f) \sin(\phi). \quad (41)$$

where  $\theta$  is the arrival angle of the acoustic wave (rad) with respect to the  $x$ -axis and  $\phi$  is the arrival angle with respect to the  $y$ -axis (rad). A value of  $\theta = \phi = 0$  corresponds to a broadside or boresight wave exciting the system. For the remainder of the paper, the exponential function with respect to time is suppressed in the equations.

The displacement fields in equations (28)–(30) are now inserted into the boundary value equations given by equations (14) through (25). Additionally, the pressure field in equation (37) and the interface equation listed as equation (27) are utilized, and the resulting equations become

$$\begin{aligned} & \lambda_1 \sum_{m=-\infty}^{m=+\infty} ik_m U_m^{(1)}(a) \exp(ik_m x) + \lambda_1 ik_y \sum_{m=-\infty}^{m=+\infty} V_m^{(1)}(a) \exp(ik_m x) + \\ & (\lambda_1 + 2\mu_1) \sum_{m=-\infty}^{m=+\infty} \frac{\partial W_m^{(1)}(a)}{\partial z} \exp(ik_m x) = K \sum_{n=-\infty}^{n=+\infty} \left[ \sum_{m=-\infty}^{m=+\infty} W_m^{(1)}(a) \exp(ik_m x) \right] \delta(x - nL), \end{aligned} \quad (42)$$

$$\mu_1 \sum_{m=-\infty}^{m=+\infty} \frac{\partial V_m^{(1)}(a)}{\partial z} \exp(ik_m x) + \mu_1 ik_y \sum_{m=-\infty}^{m=+\infty} W_m^{(1)}(a) \exp(ik_m x) = 0, \quad (43)$$

$$\mu_1 \sum_{m=-\infty}^{m=+\infty} ik_m W_m^{(1)}(a) \exp(ik_m x) + \mu_1 \sum_{m=-\infty}^{m=+\infty} \frac{\partial U_m^{(1)}(a)}{\partial z} \exp(ik_m x) = 0, \quad (44)$$

$$\begin{aligned} & \lambda_1 \sum_{m=-\infty}^{m=+\infty} ik_m U_m^{(1)}(b) \exp(ik_m x) + \lambda_1 ik_y \sum_{m=-\infty}^{m=+\infty} V_m^{(1)}(b) \exp(ik_m x) + \\ & (\lambda_1 + 2\mu_1) \sum_{m=-\infty}^{m=+\infty} \frac{\partial W_m^{(1)}(b)}{\partial z} \exp(ik_m x) = \lambda_2 \sum_{m=-\infty}^{m=+\infty} ik_m U_m^{(2)}(b) \exp(ik_m x) + \\ & \lambda_2 ik_y \sum_{m=-\infty}^{m=+\infty} V_m^{(2)}(b) \exp(ik_m x) + (\lambda_2 + 2\mu_2) \sum_{m=-\infty}^{m=+\infty} \frac{\partial W_m^{(2)}(b)}{\partial z} \exp(ik_m x), \end{aligned} \quad (45)$$

$$\begin{aligned} & \mu_1 \sum_{m=-\infty}^{m=+\infty} \frac{\partial V_m^{(1)}(b)}{\partial z} \exp(ik_m x) + \mu_1 ik_y \sum_{m=-\infty}^{m=+\infty} W_m^{(1)}(b) \exp(ik_m x) = \\ & \mu_2 \sum_{m=-\infty}^{m=+\infty} \frac{\partial V_m^{(2)}(b)}{\partial z} \exp(ik_m x) + \mu_2 ik_y \sum_{m=-\infty}^{m=+\infty} W_m^{(2)}(b) \exp(ik_m x), \end{aligned} \quad (46)$$



$$\begin{aligned}
& \mu_1 \sum_{m=-\infty}^{m=+\infty} ik_m W_m^{(1)}(b) \exp(ik_m x) + \mu_1 \sum_{m=-\infty}^{m=+\infty} \frac{\partial U_m^{(1)}(b)}{\partial z} \exp(ik_m x) = \\
& \mu_2 \sum_{m=-\infty}^{m=+\infty} ik_m W_m^{(2)}(b) \exp(ik_m x) + \mu_2 \sum_{m=-\infty}^{m=+\infty} \frac{\partial U_m^{(2)}(b)}{\partial z} \exp(ik_m x), \tag{47}
\end{aligned}$$

$$\sum_{m=-\infty}^{m=+\infty} U_m^{(1)}(b) \exp(ik_m x) = \sum_{m=-\infty}^{m=+\infty} U_m^{(2)}(b) \exp(ik_m x), \tag{48}$$

$$\sum_{m=-\infty}^{m=+\infty} V_m^{(1)}(b) \exp(ik_m x) = \sum_{m=-\infty}^{m=+\infty} V_m^{(2)}(b) \exp(ik_m x), \tag{49}$$

$$\sum_{m=-\infty}^{m=+\infty} W_m^{(1)}(b) \exp(ik_m x) = \sum_{m=-\infty}^{m=+\infty} W_m^{(2)}(b) \exp(ik_m x), \tag{50}$$

$$\begin{aligned}
& \lambda_2 \sum_{m=-\infty}^{m=+\infty} ik_m U_m^{(2)}(c) \exp(ik_m x) + \lambda_2 ik_y \sum_{m=-\infty}^{m=+\infty} V_m^{(2)}(c) \exp(ik_m x) + \\
& (\lambda_2 + 2\mu_2) \sum_{m=-\infty}^{m=+\infty} \frac{\partial W_m^{(2)}(c)}{\partial z} \exp(ik_m x) + \sum_{m=-\infty}^{m=+\infty} \left( \frac{\omega^2 \rho_f}{i\gamma_m} \right) W_m^{(2)}(c) \exp(ik_m x) \\
& = -2P_l \exp(ik_x x), \tag{51}
\end{aligned}$$

$$\mu_2 \sum_{m=-\infty}^{m=+\infty} \frac{\partial V_m^{(2)}(c)}{\partial z} \exp(ik_m x) + \mu_2 ik_y \sum_{m=-\infty}^{m=+\infty} W_m^{(2)}(c) \exp(ik_m x) = 0, \tag{52}$$

and

$$\mu_2 \sum_{m=-\infty}^{m=+\infty} ik_m W_m^{(2)}(c) \exp(ik_m x) + \mu_2 \sum_{m=-\infty}^{m=+\infty} \frac{\partial U_m^{(2)}(c)}{\partial z} \exp(ik_m x) = 0, \tag{53}$$

To eliminate the Dirac delta comb function present in equation (42), a form of the Poisson's summation formula written as

$$\sum_{n=-\infty}^{n=+\infty} \delta(x - nL) = \frac{1}{L} \sum_{n=-\infty}^{n=+\infty} \exp(i2\pi nx / L) \quad (54)$$

is used. Furthermore, the identity

$$\frac{1}{L} \sum_{n=-\infty}^{n=+\infty} \left[ \sum_{m=-\infty}^{m=+\infty} W_m^{(1)}(a) \exp(ik_m x) \right] \exp(i2\pi nx / L) = \frac{1}{L} \left[ \sum_{n=-\infty}^{n=+\infty} W_n^{(1)}(a) \right] \sum_{m=-\infty}^{m=+\infty} \exp(ik_m x) \quad (55)$$

is also applied to equation (42). This modified version of equation (42), with equations (43)–(53) are all multiplied by  $\exp(-ik_p x)$  and integrated from  $[0, L]$ . Because the exponential functions are orthogonal on this interval, the equations decouple into sets of  $m$ -indexed equations expressed as

$$\lambda_1 ik_m U_m^{(1)}(a) + \lambda_1 ik_y V_m^{(1)}(a) + (\lambda_1 + 2\mu_1) \frac{\partial W_m^{(1)}(a)}{\partial z} = \frac{K}{L} \sum_{n=-\infty}^{n=+\infty} W_n^{(1)}(a), \quad (56)$$

$$\mu_1 \frac{\partial V_m^{(1)}(a)}{\partial z} + \mu_1 ik_y W_m^{(1)}(a) = 0, \quad (57)$$

$$\mu_1 ik_m W_m^{(1)}(a) + \mu_1 \frac{\partial U_m^{(1)}(a)}{\partial z} = 0, \quad (58)$$

$$\begin{aligned} \lambda_1 ik_m U_m^{(1)}(b) + \lambda_1 ik_y V_m^{(1)}(b) + (\lambda_1 + 2\mu_1) \frac{\partial W_m^{(1)}(b)}{\partial z} = \\ \lambda_2 ik_m U_m^{(2)}(b) + \lambda_2 ik_y V_m^{(2)}(b) + (\lambda_2 + 2\mu_2) \frac{\partial W_m^{(2)}(b)}{\partial z}, \end{aligned} \quad (59)$$

$$\mu_1 \frac{\partial V_m^{(1)}(b)}{\partial z} + \mu_1 i k_y W_m^{(1)}(b) = \mu_2 \frac{\partial V_m^{(2)}(b)}{\partial z} + \mu_2 i k_y W_m^{(2)}(b), \quad (60)$$

$$\mu_1 i k_m W_m^{(1)}(b) + \mu_1 \frac{\partial U_m^{(1)}(b)}{\partial z} = \mu_2 i k_m W_m^{(2)}(b) + \mu_2 \frac{\partial U_m^{(2)}(b)}{\partial z}, \quad (61)$$

$$U_m^{(1)}(b) = U_m^{(2)}(b), \quad (62)$$

$$V_m^{(1)}(b) = V_m^{(2)}(b), \quad (63)$$

$$W_m^{(1)}(b) = W_m^{(2)}(b), \quad (64)$$

$$\lambda_2 i k_m U_m^{(2)}(c) + \lambda_2 i k_y V_m^{(2)}(c) + (\lambda_2 + 2\mu_2) \frac{\partial W_m^{(2)}(c)}{\partial z} + \left( \frac{\omega^2 \rho_f}{i \gamma_m} \right) W_m^{(2)}(c) = \begin{cases} -2P_I & m = 0 \\ 0 & m \neq 0, \end{cases} \quad (65)$$

$$\mu_2 \frac{\partial V_m^{(2)}(c)}{\partial z} + \mu_2 i k_y W_m^{(2)}(c) = 0, \quad (66)$$

and

$$\mu_2 i k_m W_m^{(2)}(c) + \mu_2 \frac{\partial U_m^{(2)}(c)}{\partial z} = 0. \quad (67)$$

The functional form of the displacements given in equations (32), (33), and (34) are inserted into equations (56)–(67) and the resulting algebraic matrix equation for each  $m$ -indexed coefficient is



$$[\mathbf{A}(k_m)]\{\mathbf{x}(k_m)\} = \sum_{n=-\infty}^{n=+\infty} [\mathbf{F}(k_n)]\{\mathbf{x}(k_n)\} + \begin{cases} \{\mathbf{p}\} & m = 0 \\ \mathbf{0} & m \neq 0 \end{cases}, \quad (68)$$

where  $[\mathbf{A}(k_m)]$  is a twelve by twelve matrix that models the dynamics of the backing plate and the acoustic coating,  $\{\mathbf{x}(k_m)\}$  is the twelve by one vector of unknown wave propagation coefficients,  $[\mathbf{F}(k_n)]$  is the twelve by twelve matrix that models the dynamic interaction of the springs and the backing plate, and  $\{\mathbf{p}\}$  is the twelve by one matrix that models the incoming acoustic wave acting on the structure. The entries of the matrices and vectors in equation (68) are listed in the appendix. Equation (68) is now written for all values of the index  $m$  and the results are inserted are rewritten in global matrix form as

$$\hat{\mathbf{A}} \hat{\mathbf{x}} = \hat{\mathbf{F}} \hat{\mathbf{x}} + \hat{\mathbf{p}}, \quad (69)$$

where  $\hat{\mathbf{A}}$  is a block diagonal matrix and is written as

$$\hat{\mathbf{A}} = \begin{bmatrix} \ddots & & \vdots & & \ddots \\ & \mathbf{A}(k_{-1}) & \mathbf{0} & \mathbf{0} & \\ \cdots & \mathbf{0} & \mathbf{A}(k_0) & \mathbf{0} & \cdots \\ & \mathbf{0} & \mathbf{0} & \mathbf{A}(k_1) & \\ \ddots & & \vdots & & \ddots \end{bmatrix}, \quad (70)$$

$\hat{\mathbf{F}}$  is a rank deficient, block partitioned matrix and is equal to

$$\hat{\mathbf{F}} = \begin{bmatrix} \ddots & & \vdots & & \ddots \\ & \mathbf{F}(k_{-1}) & \mathbf{F}(k_0) & \mathbf{F}(k_1) & \\ \cdots & \mathbf{F}(k_{-1}) & \mathbf{F}(k_0) & \mathbf{F}(k_1) & \cdots \\ & \mathbf{F}(k_{-1}) & \mathbf{F}(k_0) & \mathbf{F}(k_1) & \\ \ddots & & \vdots & & \ddots \end{bmatrix}, \quad (71)$$

$\hat{\mathbf{p}}$  is the system excitation vector and is written as

$$\hat{\mathbf{p}} = \begin{bmatrix} \cdots & \mathbf{0}^T & \mathbf{p}^T & \mathbf{0}^T & \cdots \end{bmatrix}^T, \quad (72)$$

and  $\hat{\mathbf{x}}$  is the vector that contains the unknown wave propagation coefficients and is equal to

$$\hat{\mathbf{x}} = \begin{bmatrix} \cdots & \{\mathbf{x}(k_{-1})\}^T & \{\mathbf{x}(k_0)\}^T & \{\mathbf{x}(k_1)\}^T & \cdots \end{bmatrix}^T, \quad (73)$$

where

$$\{\mathbf{x}(k_0)\} = \begin{bmatrix} A_0^{(1)} & B_0^{(1)} & C_0^{(1)} & D_0^{(1)} & E_0^{(1)} & F_0^{(1)} & \cdots \\ \cdots A_0^{(2)} & B_0^{(2)} & C_0^{(2)} & D_0^{(2)} & E_0^{(2)} & F_0^{(1)} \end{bmatrix}^T. \quad (74)$$

The  $\mathbf{0}$  term in equation (70) is a twelve by twelve matrix with all zero entries and the  $\mathbf{0}$  term in equation (72) is a twelve by one vector with all zero entries. The solution to the wave propagation coefficients is now found by truncating the matrix equation (69) to a finite number of terms and solving

$$\hat{\mathbf{x}} = [\hat{\mathbf{A}} - \hat{\mathbf{F}}]^{-1} \hat{\mathbf{p}}. \quad (75)$$

Once these are known, the displacement field of the system in the spatial domain can be determined using equations (32), (33), and (34). Furthermore, the stress distribution in the backing plate and the scattered acoustic field can be computed.

#### 4. MODEL VALIDATION

The fully elastic model that has been developed in sections 2 and 3 can be compared to a fluid-loaded, ribbed, Bernoulli-Euler thin plate that has been previously developed.<sup>7-9</sup> This will provide validation of the model for low frequencies and small plate thickness. This Bernoulli-Euler model, however, only incorporates flexural wave behavior, making the model assumptions invalid at higher frequencies and wavenumbers. The thin plate model has one degree-of-freedom that is constant displacement in the  $z$ -direction. This displacement equation is written as

$$w(x, y) = \sum_{m=-\infty}^{m=+\infty} W_m \exp(ik_m x) \exp(ik_y y) , \quad (76)$$

and this displacement field can be determined by

$$\{\mathbf{w}\} = [\mathbf{T} + \mathbf{R}]^{-1} \{\mathbf{f}\} , \quad (77)$$

where

$$\{\mathbf{w}\} = \{\dots \quad W_{-1} \quad W_0 \quad W_1 \quad \dots\}^T , \quad (78)$$

$$[\mathbf{T}] = \begin{bmatrix} \ddots & & \vdots & & \ddots \\ & T^{(-1)} & 0 & 0 & \\ \dots & 0 & T^{(0)} & 0 & \dots \\ & 0 & 0 & T^{(1)} & \\ \ddots & & \vdots & & \ddots \end{bmatrix} \quad (79)$$



$$[\mathbf{R}] = (K/L) \begin{bmatrix} \ddots & & \vdots & & \ddots \\ & & 1 & 1 & 1 \\ \cdots & 1 & 1 & 1 & \cdots \\ & & 1 & 1 & 1 \\ \ddots & & \vdots & & \ddots \end{bmatrix}, \quad (80)$$

and

$$\{\mathbf{f}\} = \{\cdots \quad 0 \quad -2P_I \quad 0 \quad \cdots\}^T. \quad (81)$$

In Eq. (79), the indexed entry is

$$T^{(n)} = D(k_n^4 + k_n^2 k_y^2 + k_y^4) - \rho h \omega^2 + (\rho_f \omega^2 / i \gamma_n), \quad (82)$$

where

$$D = \frac{Eh^3}{12(1-\nu^2)}, \quad (83)$$

where  $E$  is Young's modulus ( $\text{N m}^{-2}$ ) and  $\nu$  is Poisson's ratio (dimensionless).

Figure 2 is a plot of the magnitude of the transfer function of the plate normal displacement ( $w$ ) divided by the amplitude of the applied incident pressure field ( $P_I$ ) versus  $k_x$  wavenumber (top) and  $k_y$  wavenumber (bottom) at a frequency of 10 Hz. In the top plot, the  $k_y$  wavenumber was equal to  $2 \text{ rad m}^{-1}$  and in the bottom plot the  $k_x$  wavenumber was also equal to  $2 \text{ rad m}^{-1}$ . This extremely low frequency was chosen because it is a value at which the thick plate model should theoretically agree with the thin plate model. This example was generated using the following system parameters: total plate thickness  $h$  is 0.005 m, plate density  $\rho$  is  $1200 \text{ kg m}^{-3}$ , Lamé constants  $\lambda_1$  and  $\lambda_2$  are  $9.31 \times 10^8 \text{ N m}^{-2}$ , Lamé constants  $\mu_1$  and  $\mu_2$  are

$1.03 \times 10^8 \text{ N m}^{-2}$ , fluid density  $\rho_f$  is  $1025 \text{ kg m}^{-3}$ , fluid compressional wavespeed  $c_f$  is  $1500 \text{ m s}^{-1}$ , rib stiffness per unit length  $K$  is  $2 \times 10^4 \text{ N m}^{-2}$ , spatial location  $x$  is 0, spatial location  $y$  is 0, and rib separation distance  $L$  is 0.5 m. For the thick plate model, the plate interface region location  $b$  is -0.003 m and the output location was  $z = -h/2$ , which is -0.0025 m. In figure 2, the solid line is the fully elastic plate theory developed above and corresponds to equation (30) and the dot symbols is the Bernoulli-Euler plate theory and corresponds to equation (76). The elastic plate model was truncated to seven modes that produced an 84-by-84 system matrix and the thin plate model was truncated to 51 modes. There is almost total agreement between the two models over both wavenumber variables.

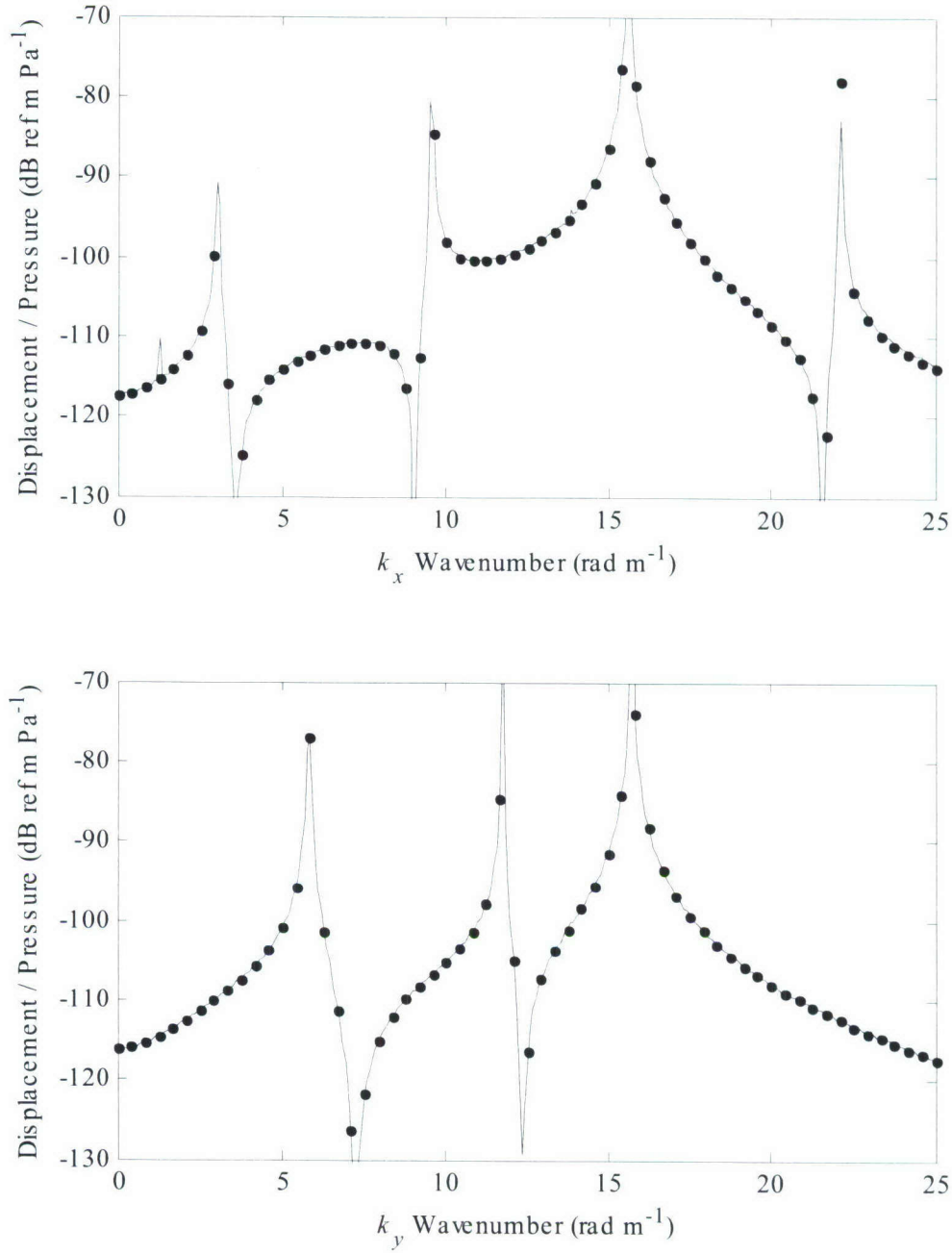


**Figure 2. Transfer Function Magnitude of Normal Displacement Divided by Incident Pressure at 10 Hz with  $k_y = 2 \text{ rad m}^{-1}$  (top) and  $k_x = 2 \text{ rad m}^{-1}$  (bottom) for Thick Plate System (—) and Thin Plate System (•)**



## 5. AN EXAMPLE PROBLEM

An example problem is now generated and discussed. This problem consists of a 0.0065-m (0.25-inch) thick aluminum plate coated with a 0.0254-m (1-inch) thick urethane polymer coating. This example was generated with the following parameters: aluminum Lamé constant  $\lambda_1$  is  $5.11 \times 10^{10} \text{ N m}^{-2}$ , Lamé constant  $\mu_1$  is  $2.63 \times 10^{10} \text{ N m}^{-2}$ , density  $\rho_1$  is  $2710 \text{ kg m}^{-3}$ , urethane Lamé constant  $\lambda_2$  is  $2.09 \times 10^9 \text{ N m}^{-2}$ , Lamé constant  $\mu_2$  is  $7.14 \times 10^7 \text{ N m}^{-2}$ , density  $\rho_2$  is  $1110 \text{ kg m}^{-3}$ , urethane structural loss factor is 0.05, fluid-compressional wavespeed  $c_f$  is  $1475 \text{ m s}^{-1}$ , fluid density  $\rho_f$  is  $1025 \text{ kg m}^{-3}$ , internal rib spacing  $L$  is 1.00 m, and rib stiffness per unit length  $K$  is  $1.20 \times 10^{10} \text{ N m}^{-2}$ . The problem is investigated from two technical standpoints: (1) the reception of an acoustic signal and (2) the echo reduction of an acoustic emission directed at the system. Because the major interest of this analysis is response to an acoustic wave in the fluid, subsequent figures are shown with respect to arrival angles rather than wavenumbers. The relationships between arrival angles and wavenumbers are given by equations (40) and (41).

The reception of an acoustic signal in the urethane can be accomplished by an internal array of sensors embedded in the coating. A typical sensor in a solid material will detect average normal stress, determined mathematically using the equation

$$\tilde{\tau}_{\text{ave}}(x, y, z_s, \omega) = \frac{\tilde{\tau}_{xx}(x, y, z_s, \omega) + \tilde{\tau}_{yy}(x, y, z_s, \omega) + \tilde{\tau}_{zz}(x, y, z_s, \omega)}{3}, \quad (84)$$

where  $z_s$  is the location of the sensors along the  $z$ -axis (m). Figure 3 is a plot of the magnitude of the average stress divided by the incident pressure versus  $\theta$  arrival angle for  $\phi$  arrival angle equal to 0 degrees (top) and average stress divided by the incident pressure versus  $\theta$  arrival angle for  $\phi$  arrival angle equal to 45 degrees (bottom) at a frequency of 8027 Hz, a value of  $y = 0$ , and a value of  $z_s = -0.0102 \text{ m}$ . In figure 3, the solid line is the fully elastic plate theory with ribs at  $x = 0$ , the long dashed line is the fully elastic plate theory with ribs at  $x = L/2$ , and the short dashed line is the fully elastic plate theory without ribs at any  $x$  value. Note that the addition of the ribs has made the stress field become spatially varying, and that different magnitudes will be present at different values of  $x$ .

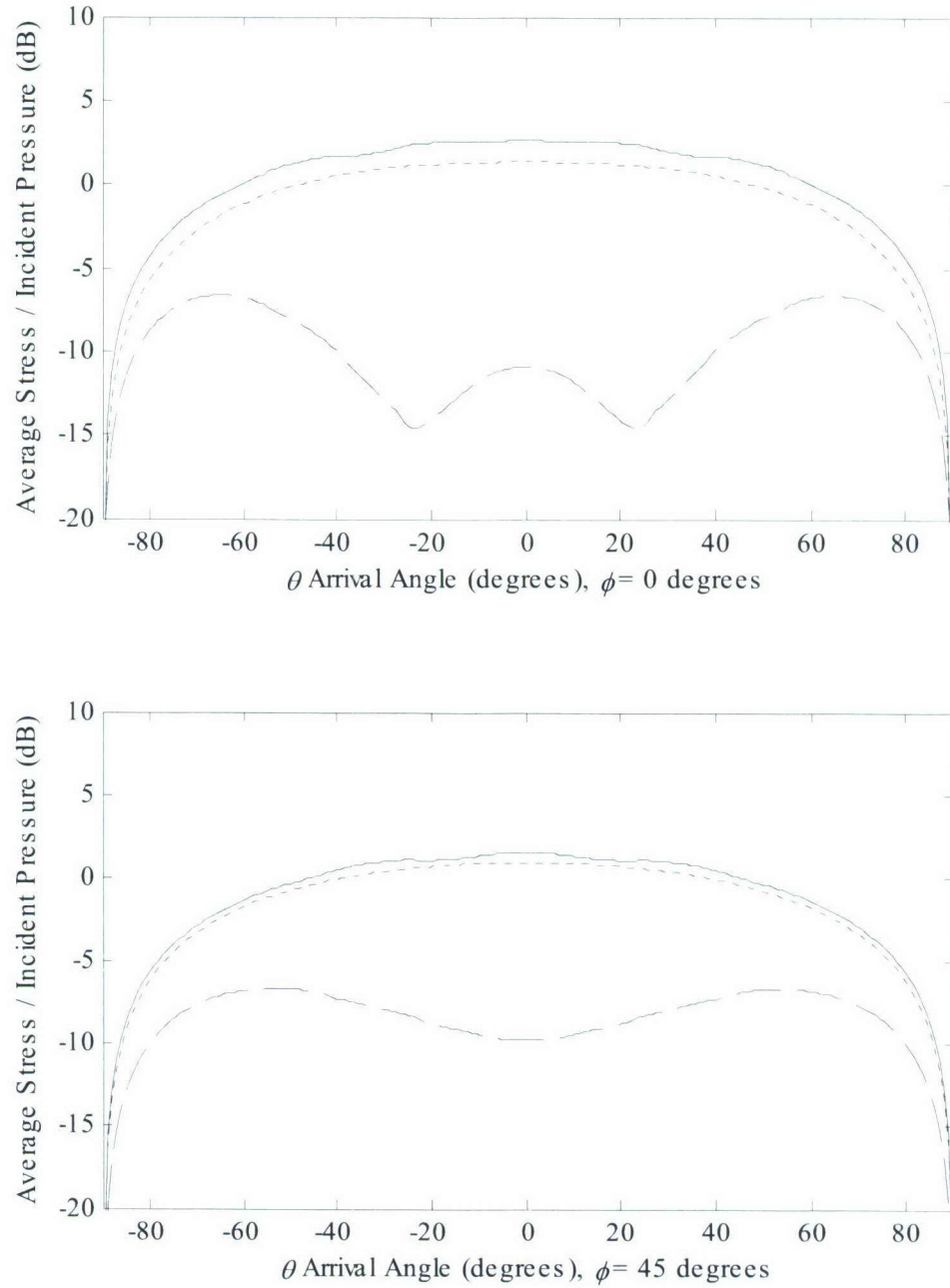


**Figure 3. Transfer Function Magnitude of Average Stress Divided by Incident Pressure at 8027 Hz with  $\phi = 0^\circ$  (top) and  $\phi = 45^\circ$  (bottom) for the System with Ribs at  $x = 0$  (\_\_\_\_),  $x = L/2$  (----) and System without Ribs at any  $x$  Value (-.-.-)**

Once the average stress field has been calculated, the summed acoustic response to an incident pressure field at fixed frequency and  $\phi = 0$  (or  $k_y = 0$ ) can be computed using

$$B(k_x, \omega) = \sum_{n=1}^N \tilde{\tau}_{\text{ave}}(x_n, 0, z_s, \omega) \exp(-ik_s x_n), \quad (85)$$

where  $N$  is the number of sensors in the array,  $k_s$  is the steered wavenumber of the array with respect to the  $x$ -axis ( $\text{rad m}^{-1}$ ), and  $x_n$  is the location of the  $n$ th sensor (m). The effect of the ribs is examined here with respect to a 16-element linear array oriented in the  $x$ -direction with an interelement spacing of 0.0625 m. Using these parameters, the summed acoustic response of the array is computed using a uniform shading function and the results are shown in figure 4. In figure 4, the top plot is the array steered to  $0^\circ$  and the bottom plot is the array steered to  $-45^\circ$ . The solid line is the array response for the system with ribs and the dashed line is the array response for the system without ribs. Note that for the array steered to  $0^\circ$  and  $-45^\circ$ , the rib structure slightly widens the beam and suppresses the maximum response. Additionally, the side lobe structure of the array response is shifted outward to a greater angle for the ribbed response. The ribs also suppress the energy in the side lobes past the second side lobe.

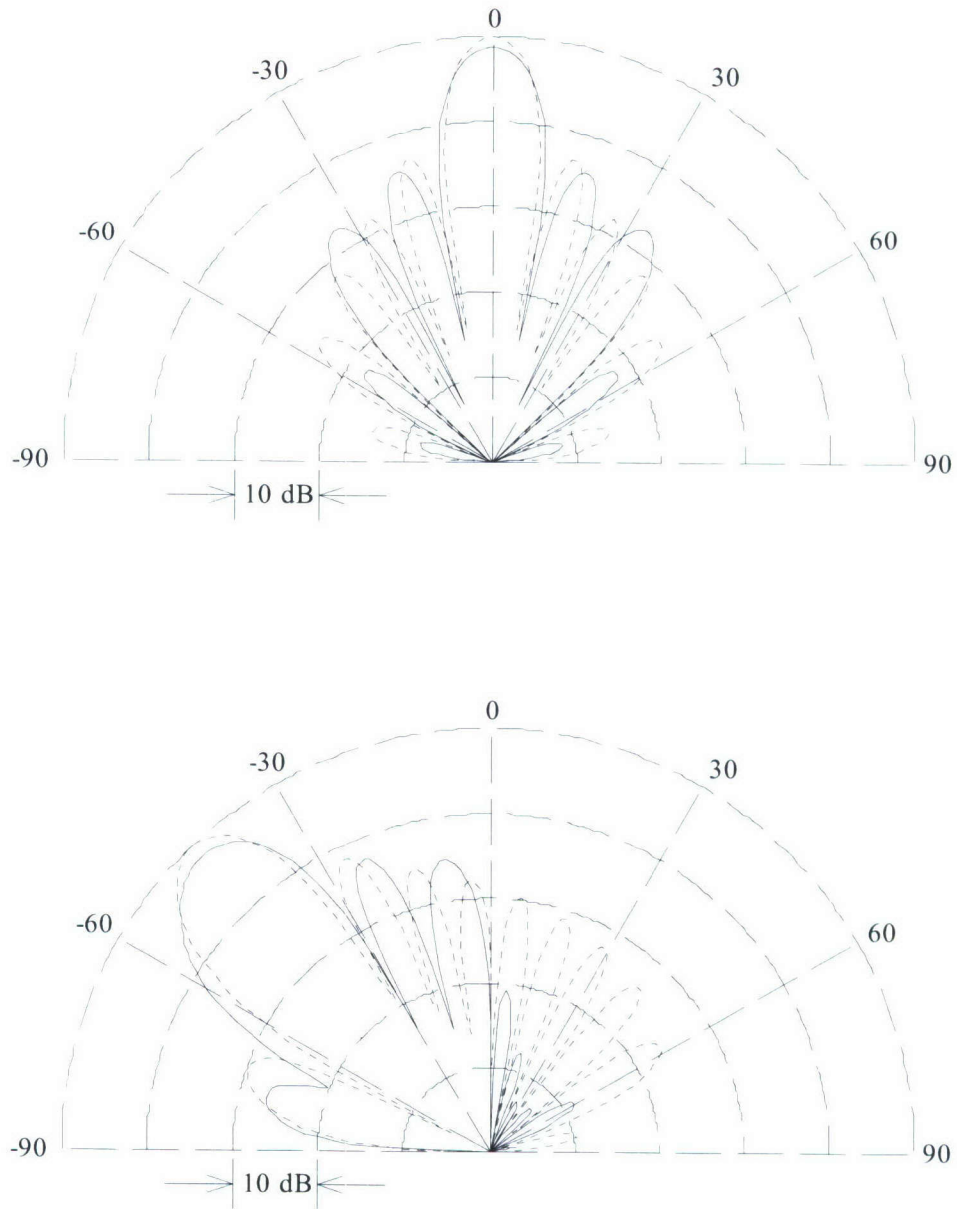


**Figure 4. Summed Acoustic Array Response with a Steer Angle of  $0^\circ$  (top) and  $-45^\circ$  (bottom) for the System with Ribs ( — ) and System without Ribs ( - - - ) at 8027 Hz**



In underwater structures, the scattered pressure field is an important quantity for quiet operation. The scattered pressure field divided by the incident pressure field is given by the expression

$$\frac{P_s(x, y, \omega)}{P_I} = \exp(ik_x x) \exp(ik_y y) + \sum_{m=-\infty}^{m=+\infty} \frac{\omega^2 \rho_f}{i \gamma_m} W_m^{(2)}(0) \exp(ik_m x) \exp(ik_y y) , \quad (86)$$

where  $P_s(x, y)$  is the scattered pressure field in the spatial-frequency domain, the first term on the right-hand side is the reflected pressure field, and the second term on the right-hand side is the radiated pressure field caused by normal displacement of the plate. Figure 5 is a plot of the magnitude of the scattered pressure divided by the incident pressure versus  $\theta$  arrival angle (top) and  $\phi$  arrival angle (bottom) at a frequency of 8027 Hz. In the top plot, the  $\phi$  arrival angle was equal to  $0^\circ$  and in the bottom plot, the  $\phi$  arrival angle was equal to  $45^\circ$ . In figure 5, the solid line is the fully elastic plate theory with ribs at  $x = 0$ , the long dashed line is the fully elastic plate theory with ribs at  $x = L/2$ , and the short dashed line is the fully elastic plate theory without ribs at any  $x$  value. The ribs add about a 2 dB spatial variation to the scattered pressure field when compared to the system without ribs. This differential is frequency dependent as it is more pronounced at various frequencies.

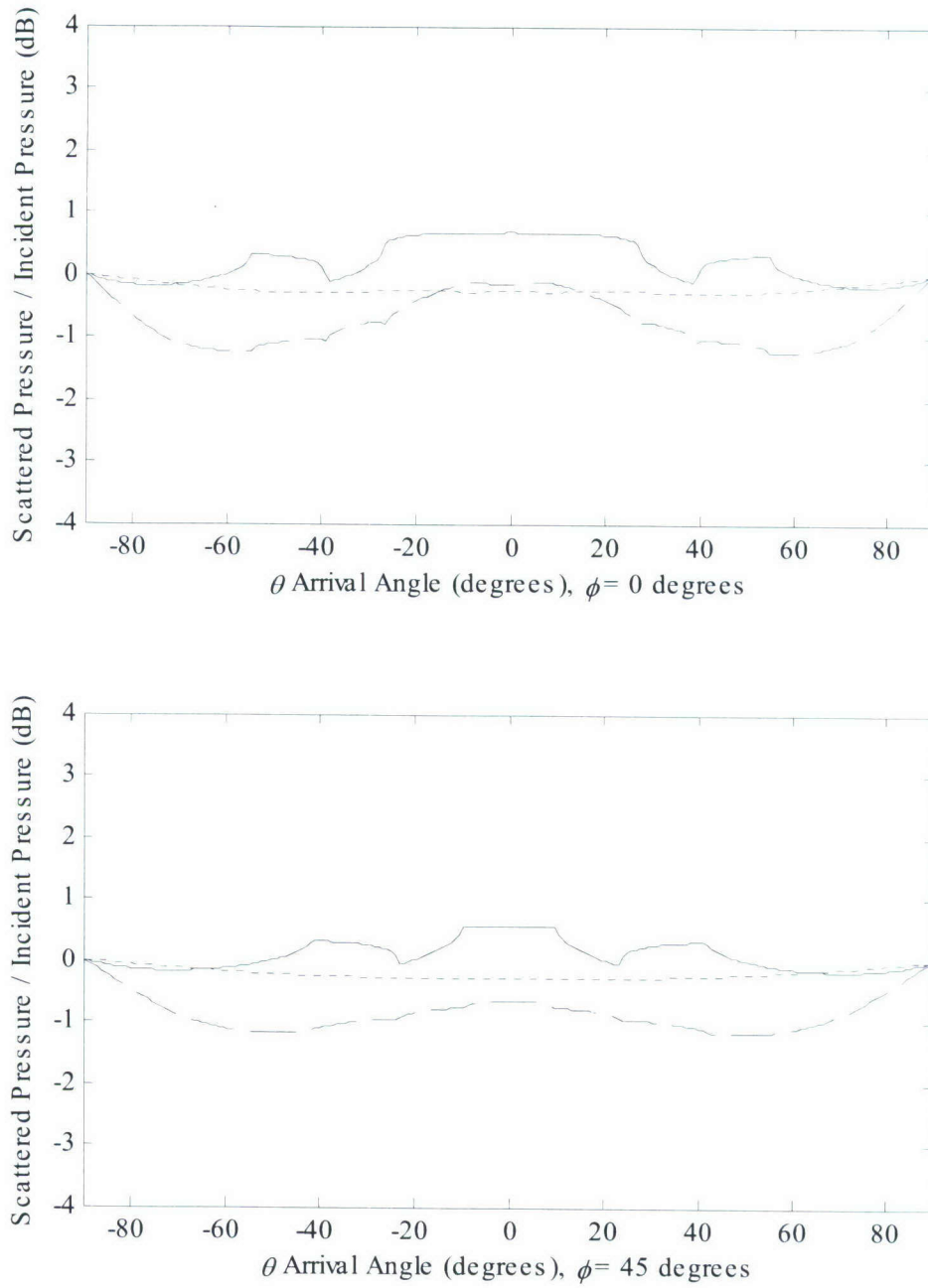


**Figure 5. Transfer Function Magnitude of Scattered Pressure Divided by Incident Pressure at 8027 Hz with  $\phi = 0^\circ$  (top) and  $\phi = 45^\circ$  (bottom) for the System with Ribs at  $x = 0$  (\_\_\_\_),  $x = L/2$  (\_\_\_\_\_) and System without Ribs at any  $x$  Value (-----)**

## 6. CONCLUSIONS

A fully elastic analytical model of a system that consists of a ribbed plate covered by a fluid-loaded acoustical coating has been derived. The model has been shown to agree with previously developed thin plate solutions to the problem at low frequency. An example problem was developed to illustrate high-frequency behavior and a comparison between the ribbed and unribbed structures is included. The specific solutions of embedded sonar system performance and scattered pressure field were investigated. It was shown that the ribs have a moderate effect on the high frequency dynamic response of the structure.

## 7. REFERENCES

1. S. M. Han, H. Benaroya, and T. Wei, "Dynamics of Transversely Vibrating Beams Using Four Engineering Theories," *Journal of Sound and Vibration*, vol. 225, no. 5, 1999, pp. 935–988.
2. R. D. Mindlin, "Influence of Rotary Inertia and Shear on Flexural Motions of Isotropic Plates," *Journal of Applied Mechanics*, vol. 18, 1951, pp. 31–38.
3. L. M Brekhovskikh, "Waves in Layered Media," Academic Press, San Diego, CA, 1980.
4. D. G. Crighton, "The Free and Forced Waves on a Fluid-Loaded Elastic Plate," *Journal of Sound and Vibration*, vol. 63, no. 2, 1979, pp. 225–235.
5. D. L. Folds and C.D. Loggins, "Transmission and Reflection of Ultrasonic Waves in Layered Media," *Journal of the Acoustical Society of America*, vol. 62, no. 5, 1977, pp. 1102–1109.
6. D. J. Mead and K. K. Pujara, "Space-Harmonic Analysis of a Periodically Supported Beam: Response to Convected Random Loading," *Journal of Sound and Vibration*, vol. 14, no. 4, 1971, pp. 525–541.
7. B. R. Mace, "Periodically Stiffened Fluid-Loaded Plates, I: Response to Convected Harmonic Pressure and Free Wave Propagation," *Journal of Sound and Vibration*, vol. 73, no. 4, 1980, pp. 473–486.
8. B. R. Mace, "Periodically Stiffened Fluid-Loaded Plates, II: Response to Line and Point Forces," *Journal of Sound and Vibration*, vol. 73, no. 4, 1980, pp. 487–504.
9. B. A. Cray, "Acoustic Radiation from Periodic and Sectionally Aperiodic Rib-Stiffened Plates," *Journal of the Acoustical Society of America*, vol. 95, no. 1, 1994, pp. 256–264.



10. G. P. Eatwell and D. Butler, "The Response of Fluid-Loaded, Beam-Stiffened Plates," *Journal of Sound and Vibration*, vol. 84, no. 3, 1982, pp. 371–388.
11. G. P. Eatwell, "Free-Wave Propagation in an Irregularly Stiffened, Fluid Loaded Plate," *Journal of Sound and Vibration*, vol. 88, no. 4, 1983, pp. 507–522.
12. C. J. Chapman and S. V. Sorokin, "The Forced Vibration of an Elastic Plate Under Significant Fluid Loading," *Journal of Sound and Vibration*, vol. 281, nos. 3–5, 2005, pp. 719–741.
13. S. H. Ko, W. Seong, and S. Pyo, "Structureborne Noise Reduction for an Infinite, Elastic Cylindrical Shell," *Journal of the Acoustical Society of America*, vol. 109, no. 4, 2001, pp. 1483–1495.
14. J. M. Cuschieri and D. Feit, "Influence of Circumferential Partial Coating on the Acoustic Radiation from a Fluid-Loaded Shell," *Journal of the Acoustical Society of America*, vol. 107, no. 6, 2000, pp. 3196–3207.
15. W. Zhang, A. Wang, N. Vlahopoulos, and K. Wu, "High-Frequency Vibration Analysis of Thin Elastic Plates Under Heavy Fluid Loading by an Energy Finite Element Formulation," *Journal of Sound and Vibration*, vol. 263, no. 1, 2003, pp. 21–46.
16. A. J. Hull, "Dynamic Response of an Elastic Plate Containing Periodic Masses," *Journal of Sound and Vibration*, vol. 310 nos. 1–2, 2008, pp. 1–20.

## APPENDIX MATRIX AND VECTOR ENTRIES

The entries of the matrixes and vectors in equation (75) are listed below. Without loss of generality, the top of the top plate is defined as  $z = c = 0$ . For the  $[\mathbf{A}(k_n)]$  matrix, the nonzero entries are

$$a_{1,1} = \{-\lambda_1[(\alpha_n^{(1)})^2 + k_n^2 + k_y^2] - 2\mu_1(\alpha_n^{(1)})^2\} \cos(\alpha_n^{(1)}a), \quad (\text{A-1})$$

$$a_{1,2} = \{-\lambda_1[(\alpha_n^{(1)})^2 + k_n^2 + k_y^2] - 2\mu_1(\alpha_n^{(1)})^2\} \sin(\alpha_n^{(1)}a), \quad (\text{A-2})$$

$$a_{1,3} = 2i\mu_1\beta_n^{(1)}k_y \sin(\beta_n^{(1)}a), \quad (\text{A-3})$$

$$a_{1,4} = -2i\mu_1\beta_n^{(1)}k_y \cos(\beta_n^{(1)}a), \quad (\text{A-4})$$

$$a_{1,5} = -2i\mu_1\beta_n^{(1)}k_n \sin(\beta_n^{(1)}a), \quad (\text{A-5})$$

$$a_{1,6} = 2i\mu_1\beta_n^{(1)}k_n \cos(\beta_n^{(1)}a), \quad (\text{A-6})$$

$$a_{2,1} = -2i\mu_1\alpha_n^{(1)}k_y \sin(\alpha_n^{(1)}a), \quad (\text{A-7})$$

$$a_{2,2} = 2i\mu_1\alpha_n^{(1)}k_y \cos(\alpha_n^{(1)}a), \quad (\text{A-8})$$

$$a_{2,3} = -\mu_1[(\beta_n^{(1)})^2 + k_n^2 - k_y^2] \cos(\beta_n^{(1)}a), \quad (\text{A-9})$$

$$a_{2,4} = -\mu_1[(\beta_n^{(1)})^2 + k_n^2 - k_y^2] \sin(\beta_n^{(1)}a), \quad (\text{A-10})$$

$$a_{2,5} = -2\mu_1 k_y k_n \cos(\beta_n^{(1)} a), \quad (\text{A-11})$$

$$a_{2,6} = -2\mu_1 k_y k_n \sin(\beta_n^{(1)} a), \quad (\text{A-12})$$

$$a_{3,1} = -2i\mu_1 \alpha_n^{(1)} k_n \sin(\alpha_n^{(1)} a), \quad (\text{A-13})$$

$$a_{3,2} = 2i\mu_1 \alpha_n^{(1)} k_n \cos(\alpha_n^{(1)} a), \quad (\text{A-14})$$

$$a_{3,3} = \mu_1 k_n k_y [\cos(\beta_n^{(1)} a) - \sin(\beta_n^{(1)} a)], \quad (\text{A-15})$$

$$a_{3,4} = \mu_1 k_n k_y [\sin(\beta_n^{(1)} a) - \cos(\beta_n^{(1)} a)], \quad (\text{A-16})$$

$$a_{3,5} = \mu_1 [(\beta_n^{(1)})^2 - k_n^2] \cos(\beta_n^{(1)} a) - \mu_1 k_y^2 \sin(\beta_n^{(1)} a), \quad (\text{A-17})$$

$$a_{3,6} = \mu_1 [(\beta_n^{(1)})^2 - k_n^2] \sin(\beta_n^{(1)} a) - \mu_1 k_y^2 \cos(\beta_n^{(1)} a), \quad (\text{A-18})$$

$$a_{4,1} = \{-\lambda_1 [(\alpha_n^{(1)})^2 + k_n^2 + k_y^2] - 2\mu_1 (\alpha_n^{(1)})^2\} \cos(\alpha_n^{(1)} b), \quad (\text{A-19})$$

$$a_{4,2} = \{-\lambda_1 [(\alpha_n^{(1)})^2 + k_n^2 + k_y^2] - 2\mu_1 (\alpha_n^{(1)})^2\} \sin(\alpha_n^{(1)} b), \quad (\text{A-20})$$

$$a_{4,3} = 2i\mu_1 \beta_n^{(1)} k_y \sin(\beta_n^{(1)} b), \quad (\text{A-21})$$

$$a_{4,4} = -2i\mu_1 \beta_n^{(1)} k_y \cos(\beta_n^{(1)} b), \quad (\text{A-22})$$

$$a_{4,5} = -2i\mu_1\beta_n^{(1)}k_n \sin(\beta_n^{(1)}b), \quad (\text{A-23})$$

$$a_{4,6} = 2i\mu_1\beta_n^{(1)}k_n \cos(\beta_n^{(1)}b), \quad (\text{A-24})$$

$$a_{4,7} = \{\lambda_2[(\alpha_n^{(2)})^2 + k_n^2 + k_y^2] + 2\mu_2(\alpha_n^{(2)})^2\} \cos(\alpha_n^{(2)}b), \quad (\text{A-25})$$

$$a_{4,8} = \{\lambda_2[(\alpha_n^{(2)})^2 + k_n^2 + k_y^2] + 2\mu_2(\alpha_n^{(2)})^2\} \sin(\alpha_n^{(2)}b), \quad (\text{A-26})$$

$$a_{4,9} = -2i\mu_2\beta_n^{(2)}k_y \sin(\beta_n^{(2)}b), \quad (\text{A-27})$$

$$a_{4,10} = 2i\mu_2\beta_n^{(2)}k_y \cos(\beta_n^{(2)}b), \quad (\text{A-28})$$

$$a_{4,11} = 2i\mu_2\beta_n^{(2)}k_n \sin(\beta_n^{(2)}b), \quad (\text{A-29})$$

$$a_{4,12} = -2i\mu_2\beta_n^{(2)}k_n \cos(\beta_n^{(2)}b), \quad (\text{A-30})$$

$$a_{5,1} = -2i\mu_1\alpha_n^{(1)}k_y \sin(\alpha_n^{(1)}b), \quad (\text{A-31})$$

$$a_{5,2} = 2i\mu_1\alpha_n^{(1)}k_y \cos(\alpha_n^{(1)}b), \quad (\text{A-32})$$

$$a_{5,3} = -\mu_1[(\beta_n^{(1)})^2 + k_n^2 - k_y^2] \cos(\beta_n^{(1)}b), \quad (\text{A-33})$$

$$a_{5,4} = -\mu_1[(\beta_n^{(1)})^2 + k_n^2 - k_y^2] \sin(\beta_n^{(1)}b), \quad (\text{A-34})$$

$$a_{5,5} = -2\mu_1k_yk_n \cos(\beta_n^{(1)}b), \quad (\text{A-35})$$



$$a_{5,6} = -2\mu_1 k_y k_n \sin(\beta_n^{(1)} b), \quad (\text{A-36})$$

$$a_{5,7} = 2i\mu_2 \alpha_n^{(2)} k_y \sin(\alpha_n^{(2)} b), \quad (\text{A-37})$$

$$a_{5,8} = -2i\mu_2 \alpha_n^{(2)} k_y \cos(\alpha_n^{(2)} b), \quad (\text{A-38})$$

$$a_{5,9} = \mu_2 [(\beta_n^{(2)})^2 + k_n^2 - k_y^2] \cos(\beta_n^{(2)} b), \quad (\text{A-39})$$

$$a_{5,10} = \mu_2 [(\beta_n^{(2)})^2 + k_n^2 - k_y^2] \sin(\beta_n^{(2)} b), \quad (\text{A-40})$$

$$a_{5,11} = 2\mu_2 k_y k_n \cos(\beta_n^{(2)} b), \quad (\text{A-41})$$

$$a_{5,12} = 2\mu_2 k_y k_n \sin(\beta_n^{(2)} b), \quad (\text{A-42})$$

$$a_{6,1} = -2i\mu_1 \alpha_n^{(1)} k_n \sin(\alpha_n^{(1)} b), \quad (\text{A-43})$$

$$a_{6,2} = 2i\mu_1 \alpha_n^{(1)} k_n \cos(\alpha_n^{(1)} b), \quad (\text{A-44})$$

$$a_{6,3} = \mu_1 k_n k_y [\cos(\beta_n^{(1)} b) - \sin(\beta_n^{(1)} b)], \quad (\text{A-45})$$

$$a_{6,4} = \mu_1 k_n k_y [\sin(\beta_n^{(1)} b) - \cos(\beta_n^{(1)} b)], \quad (\text{A-46})$$

$$a_{6,5} = \mu_1 [(\beta_n^{(1)})^2 - k_n^2] \cos(\beta_n^{(1)} b) - \mu_1 k_y^2 \sin(\beta_n^{(1)} b), \quad (\text{A-47})$$

$$a_{6,6} = \mu_1[(\beta_n^{(1)})^2 - k_n^2] \sin(\beta_n^{(1)} b) - \mu_1 k_y^2 \cos(\beta_n^{(1)} b), \quad (\text{A-48})$$

$$a_{6,7} = 2i\mu_2 \alpha_n^{(2)} k_n \sin(\alpha_n^{(2)} b), \quad (\text{A-49})$$

$$a_{6,8} = -2i\mu_2 \alpha_n^{(2)} k_n \cos(\alpha_n^{(2)} b), \quad (\text{A-50})$$

$$a_{6,9} = -\mu_2 k_n k_y [\cos(\beta_n^{(2)} b) - \sin(\beta_n^{(2)} b)], \quad (\text{A-51})$$

$$a_{6,10} = -\mu_2 k_n k_y [\sin(\beta_n^{(2)} b) - \cos(\beta_n^{(2)} b)], \quad (\text{A-52})$$

$$a_{6,11} = -\mu_2[(\beta_n^{(2)})^2 - k_n^2] \cos(\beta_n^{(2)} b) + \mu_2 k_y^2 \sin(\beta_n^{(2)} b), \quad (\text{A-53})$$

$$a_{6,12} = -\mu_2[(\beta_n^{(2)})^2 - k_n^2] \sin(\beta_n^{(2)} b) + \mu_2 k_y^2 \cos(\beta_n^{(2)} b), \quad (\text{A-54})$$

$$a_{7,1} = ik_n \cos(\alpha_n^{(1)} b), \quad (\text{A-55})$$

$$a_{7,2} = ik_n \sin(\alpha_n^{(1)} b), \quad (\text{A-56})$$

$$a_{7,3} = \frac{k_n k_y}{\beta_n^{(1)}} \sin(\beta_n^{(1)} b), \quad (\text{A-57})$$

$$a_{7,4} = \frac{-k_n k_y}{\beta_n^{(1)}} \cos(\beta_n^{(1)} b), \quad (\text{A-58})$$

$$a_{7,5} = \left( \beta_n^{(1)} + \frac{k_y^2}{\beta_n^{(1)}} \right) \sin(\beta_n^{(1)} b), \quad (\text{A-59})$$

$$a_{7,6} = -\left(\beta_n^{(1)} + \frac{k_y^2}{\beta_n^{(1)}}\right) \cos(\beta_n^{(1)} b), \quad (\text{A-60})$$

$$a_{7,7} = -ik_n \cos(\alpha_n^{(2)} b), \quad (\text{A-61})$$

$$a_{7,8} = -ik_n \sin(\alpha_n^{(2)} b), \quad (\text{A-62})$$

$$a_{7,9} = \frac{-k_n k_y}{\beta_n^{(2)}} \sin(\beta_n^{(2)} b), \quad (\text{A-63})$$

$$a_{7,10} = \frac{k_n k_y}{\beta_n^{(2)}} \cos(\beta_n^{(2)} b), \quad (\text{A-64})$$

$$a_{7,11} = -\left(\beta_n^{(2)} + \frac{k_y^2}{\beta_n^{(2)}}\right) \sin(\beta_n^{(2)} b), \quad (\text{A-65})$$

$$a_{7,12} = \left(\beta_n^{(2)} + \frac{k_y^2}{\beta_n^{(2)}}\right) \cos(\beta_n^{(2)} b), \quad (\text{A-66})$$

$$a_{8,1} = ik_y \cos(\alpha_n^{(1)} b), \quad (\text{A-67})$$

$$a_{8,2} = ik_y \sin(\alpha_n^{(1)} b), \quad (\text{A-68})$$

$$a_{8,3} = -\left(\beta_n^{(1)} + \frac{k_n^2}{\beta_n^{(1)}}\right) \sin(\beta_n^{(1)} b), \quad (\text{A-69})$$

$$a_{8,4} = \left( \beta_n^{(1)} + \frac{k_n^2}{\beta_n^{(1)}} \right) \cos(\beta_n^{(1)} b), \quad (\text{A-70})$$

$$a_{8,5} = \frac{-k_n k_y}{\beta_n^{(1)}} \sin(\beta_n^{(1)} b), \quad (\text{A-71})$$

$$a_{8,6} = \frac{k_n k_y}{\beta_n^{(1)}} \cos(\beta_n^{(1)} b), \quad (\text{A-72})$$

$$a_{8,7} = -ik_y \cos(\alpha_n^{(2)} b), \quad (\text{A-73})$$

$$a_{8,8} = -ik_y \sin(\alpha_n^{(2)} b), \quad (\text{A-74})$$

$$a_{8,9} = \left( \beta_n^{(2)} + \frac{k_n^2}{\beta_n^{(2)}} \right) \sin(\beta_n^{(2)} b), \quad (\text{A-75})$$

$$a_{8,10} = - \left( \beta_n^{(2)} + \frac{k_n^2}{\beta_n^{(2)}} \right) \cos(\beta_n^{(2)} b), \quad (\text{A-76})$$

$$a_{8,11} = \frac{k_n k_y}{\beta_n^{(2)}} \sin(\beta_n^{(2)} b), \quad (\text{A-77})$$

$$a_{8,12} = \frac{-k_n k_y}{\beta_n^{(2)}} \cos(\beta_n^{(2)} b), \quad (\text{A-78})$$



$$a_{9,1} = -\alpha_n^{(1)} \sin(\alpha_n^{(1)} b), \quad (\text{A-79})$$

$$a_{9,2} = \alpha_n^{(1)} \cos(\alpha_n^{(1)} b), \quad (\text{A-80})$$

$$a_{9,3} = -ik_y \cos(\beta_n^{(1)} b), \quad (\text{A-81})$$

$$a_{9,4} = -ik_y \sin(\beta_n^{(1)} b), \quad (\text{A-82})$$

$$a_{9,5} = ik_n \cos(\beta_n^{(1)} b), \quad (\text{A-83})$$

$$a_{9,6} = ik_n \sin(\beta_n^{(1)} b), \quad (\text{A-84})$$

$$a_{9,7} = \alpha_n^{(2)} \sin(\alpha_n^{(2)} b), \quad (\text{A-85})$$

$$a_{9,8} = -\alpha_n^{(2)} \cos(\alpha_n^{(2)} b), \quad (\text{A-86})$$

$$a_{9,9} = ik_y \cos(\beta_n^{(2)} b), \quad (\text{A-87})$$

$$a_{9,10} = ik_y \sin(\beta_n^{(2)} b), \quad (\text{A-88})$$

$$a_{9,11} = -ik_n \cos(\beta_n^{(2)} b), \quad (\text{A-89})$$

$$a_{9,12} = -ik_n \sin(\beta_n^{(2)} b), \quad (\text{A-90})$$

$$a_{10,7} = -\lambda_2 [(\alpha_n^{(2)})^2 + k_n^2 + k_y^2] - 2\mu_2 (\alpha_n^{(2)})^2, \quad (\text{A-91})$$

$$a_{10,8} = \frac{\omega^2 \rho_f \alpha_n^{(2)}}{i\gamma_n}, \quad (\text{A-92})$$

$$a_{10,9} = \frac{-\omega^2 \rho_f k_y}{\gamma_n}, \quad (\text{A-93})$$

$$a_{10,10} = -2i\mu_2 \beta_n^{(2)} k_y, \quad (\text{A-94})$$

$$a_{10,11} = \frac{\omega^2 \rho_f k_n}{\gamma_n}, \quad (\text{A-95})$$

$$a_{10,12} = 2i\mu_2 \beta_n^{(2)} k_n, \quad (\text{A-96})$$

$$a_{11,8} = 2i\mu_2 \alpha_n^{(2)} k_y, \quad (\text{A-97})$$

$$a_{11,9} = -\mu_2 (\beta_n^{(2)} + k_n^2 - k_y^2), \quad (\text{A-98})$$

$$a_{11,11} = -2\mu_2 k_n k_y, \quad (\text{A-99})$$

$$a_{12,8} = 2i\mu_2 \alpha_n^{(2)} k_n, \quad (\text{A-100})$$

$$a_{12,9} = \mu_2 k_n k_y, \quad (\text{A-101})$$

$$a_{12,10} = -\mu_2 k_n k_y, \quad (\text{A-102})$$

$$a_{12,11} = \mu_2 [(\beta_n^{(2)})^2 - k_n^2], \quad (\text{A-103})$$

and

$$a_{12,12} = -\mu_2 k_y^2. \quad (\text{A-104})$$

The nonzero entries of the  $[\mathbf{F}(k_n)]$  matrix are

$$f_{1,1} = -(K/L) \alpha_n^{(1)} \sin(\alpha_n^{(1)} a), \quad (\text{A-105})$$

$$f_{1,2} = (K/L) \alpha_n^{(1)} \cos(\alpha_n^{(1)} a), \quad (\text{A-106})$$

$$f_{1,3} = -(K/L) i k_y \cos(\beta_n^{(1)} a), \quad (\text{A-107})$$

$$f_{1,4} = -(K/L) i k_y \sin(\beta_n^{(1)} a), \quad (\text{A-108})$$

$$f_{1,5} = (K/L) i k_n \cos(\beta_n^{(1)} a), \quad (\text{A-109})$$

and

$$f_{1,6} = (K/L) i k_n \sin(\beta_n^{(1)} a). \quad (\text{A-110})$$

The entries of the  $\mathbf{p}$  vector are

$$\mathbf{p} = [0 \quad 0 \quad 0 \quad 0 \quad 0 \quad 0 \quad 0 \quad 0 \quad 0 \quad 0 \quad -2P_I \quad 0 \quad 0]^T. \quad (\text{A-111})$$

## INITIAL DISTRIBUTION LIST

Addressee	No. of Copies
Office of Naval Research (Code 333—R. Soukup; 331—L. Couchman; 321—M. Traweck)	3
Defense Technical Information Center	2
Center for Naval Analyses	1